Int. J. Electrochem. Sci., 17 **(2022)** Article Number: 22074, doi: 10.20964/2022.07.27

International Journal of
ELECTROCHEMICAL
SCIENCE
www.electrochemsci.org

Application of Taylor's series with Ying Buzu Shu algorithm for the nonlinear problem in amperometric biosensors

B. Manimegalai[1], R Swaminathan[2], Michael E.G. Lyons[3,], L. Rajendran[1,*]*

[1] Department of Mathematics, AMET Deemed to be University, Kanathur, Chennai-603112, India
[2] Department of Mathematics, Vidhyaa Giri College of Arts and Science, Sivaganga - 630108, India
[3] School of Chemistry & AMBER National Centre, University of Dublin, Trinity College Dublin, Dublin 2, Ireland
[*]E-mail: melyons@tcd.ie (MEG Lyons); raj_sms@rediffmail.com (L.Rajendran)

Received: 5 January 2022 / *Accepted:* 13 February 2022 / *Published:* 6 June 2022

The enzyme combines with an electroinactive substrate to produce an electroactive product that is oxidised or reduced rapidly at the electrode/film interface in this method. This model is built on nonlinear reaction-diffusion equations containing a nonlinear factor related to the enzyme reaction's Michaelis-Menten kinetics. In this paper, the Taylor's series method with the ancient Chinese algorithm (Ying Buzu Shu algorithm) is applied to derive an analytical solution for the nonlinear problems in amperometric biosensors. Finally, simple and closed-form analytical expressions for the steady-state concentration profiles and their related current response in enzyme immobilized into a planar film onto an electrode are derived. The analytical concentration profiles are compared with the simulation and gave a satisfactory agreement.

Keywords: Michaelis–Menten kinetics; Amperometric biosensor; Nonlinear reaction-diffusion equations; Taylor's series method; Ying Buzu Shu algorithm

1. INTRODUCTION

Biosensors are self-contained analytical devices that turn biological responses into quantifiable and processable signals, which is also a self-contained integrated device that incorporates a biological recognition element with a physical transducer. The biosensor can be classified into electrochemical, optical, thermal, and piezoelectric based on the transducer. Moreover, Electrochemical biosensors are of three types called amperometric biosensors, potentiometric biosensors and conductometric biosensors. The current produced during the oxidation or reduction of an electroactive product or reactant is measured using an amperometric biosensor. The potential of the biosensor electrode with a reference

electrode is calculated using a potentiometric biosensor. Finally, the conductance change caused by a biological reaction is measured using conductometric biosensors.

Electrochemical biosensors have been the most extensively studied due to their low detection limit, specificity, ease of manufacture, and operation. The electrochemical oxidation (or reduction) of the substrate catalysed by enzymes to produce catalytic currents is known as bioelectrocatalysis. The current response of mediated amperometric biosensors is based on this principle, and numerous research articles have been published on this topic. By using redox chemicals as electron transfer mediators, enzymes on electrodes catalyzed electrolytic oxidations or reductions of substrates. The importance of bioelectrocatalysis extends beyond biosensor applications. It's also used to design energy devices like bioreactors [1] and biofuel cells [2]. For environmental, clinical, and industrial reasons, these are reliable, inexpensive, and very sensitive. As a result, mathematical modelling of the situation is quite beneficial.

Using Danckwert's formula, Rajendran and Rahamathunissa [3] calculate the analytical solution of steady-state current for amperometric polymer electrodes in first- and zero-order kinetics. Eswari and Rajendran [4] measured the steady-state concentration and current at the microdisk and microcylinder electrodes for an amperometric biosensor. The homotopy perturbation method was utilized by Rajendran and Anitha [5] to solve the nonlinear mass balance equation in the amperometric biosensor.

Although there is considerable overlap between biosensors and enzymatic electrodes for fuel cell applications, Bartlett et al. [6] provide a thorough examination of the problem. Britz et al. [7] show how to simulate chronoamperometry on an electrode with a thin enzyme layer using algorithms. The mathematical model [8] was recently constructed based on substrate enzymatic conversion and substrate diffusion. Meena et al. [9] investigated the mathematical model of the amperometric and potentiometric biosensor in non-steady-state situations using the homotopy perturbation method. The numerical and analytical models of amperometric and potentiometric enzyme electrodes and reactors was developed by Morf and colleagues [10,11]. With a focus on the influence of catalytic activity and biosensor shape, Aseris et al. [12] examined the operation of a biosensor by changing input parameters.The substrate and inhibitor of an amperometric biosensor response model was developed by Achi et al. [13]. The non-linear reaction-diffusion equations in a mono-enzymatic biosensor were solved by Kirthiga and Rajendran [14] using the homotopy analysis method.

However, there are no defined criteria for constructing electrochemical biosensors, biofuel cells, or bioreactors that use immobilized enzymes. Using Taylor’s series with the Chinese algorithm called Ying Buzu Shu algorithm, we have derived approximate analytical expressions of concentrations and current density, which can be used to describe and evaluate the performance of energy devices. The numerical results correspond well with the new simple and closed-form of our approximate analytical expression for steady-state substrate and product concentrations.

2. MATHEMATICAL FORMULATION OF THE PROBLEM

The chemical reactions that occur in the layer are as follows:

$$E + S \leftrightarrow ES \rightarrow E + P \quad (1)$$

where E is the enzyme, S is the substrate, ES is an enzyme substrate complex and P is the product.

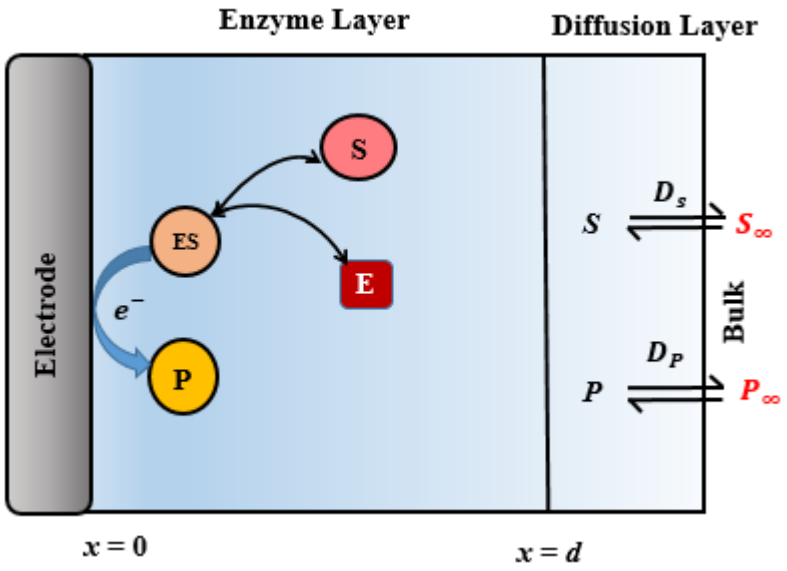

Figure 1. Schematic diagram for an amperometric biosensor

For a steady-state mono-enzymatic biosensor, the mass balance equations to describe the diffusion of the substrate *S* and product *P* are shown below [14]:

$$D_S \frac{d^2[S](x)}{dx^2} - V_m \frac{[S](x)}{K_m + [S](x)} = 0 \quad (2)$$

$$D_P \frac{d^2[P](x)}{dx^2} + V_m \frac{[S](x)}{K_m + [S](x)} = 0 \quad (3)$$

where D_S and D_P denote the diffusion coefficients, V_m is the maximum enzymatic reaction rate and K_m is the Michaelis–Menten constant. The boundary conditions for the above equations are as follows:

$$\text{At } x = 0, \frac{d[S]}{dx} = 0; [P] = 0 \quad (4)$$

$$\text{At } x = d, [S] = S_0; [P] = 0 \quad (5)$$

Current density *J* [14], which occurs at the electrode due to reduction or oxidation of *P*, is given as follows:

$$J = n_e F D_P \left(\frac{d[P]}{dx}\right)_{x=0} \quad (6)$$

The dimensionless forms of the above equations (2-6) becomes as follows:

$$\frac{d^2u(\chi)}{d\chi^2} - \frac{\mu u(\chi)}{\kappa + u(\chi)} = 0 \quad (7)$$

$$\gamma \frac{d^2v(\chi)}{d\chi^2} + \frac{\mu u(\chi)}{\kappa + u(\chi)} = 0 \quad (8)$$

where,

$$u(\chi) = \frac{S(x)}{S_0}, v(\chi) = \frac{P(x)}{S_0}, \chi = \frac{x}{d}, \mu = \frac{V_m d^2}{D_s S_0}, \kappa = \frac{K_m}{S_0}, \gamma = \frac{D_p}{D_s} \quad (9)$$

The respective boundary conditions are

$$\text{At } \chi = 0, \frac{du}{d\chi} = 0, v = 0 \tag{10}$$

$$\text{At } \chi = 1, u = 1, v = 0 \tag{11}$$

The dimensionless current is reduced to

$$\psi = \frac{Jd}{n_e F D_p S_0} = \left.\frac{dv(\chi)}{d\chi}\right|_{\chi=0} \tag{12}$$

3. ANALYTICAL EXPRESSION OF THE CONCENTRATIONS USING TAYLOR'S SERIES WITH YING BUZU SHU ALGORITHM

The approximate methods such as homotopy perturbation method [22,23], variational iteration method [24], Akbari Ganji's method [25,26], Pade approximant method [27], Taylor's series method [28,29] are available to solve the nonlinear [30-32] differential equations. It was also mentioned that approximate analytical solutions, rather than numerical solutions, are more instructive regarding the controlling system's properties. As a result, we provide extremely reliable and accurate approximate analytical solutions in this section based on a new Taylor's series method. The approximate analytical solutions for the concentration of the substrate and product using the Taylor's series method are as follows [Appendix A-B]:

$$u(\chi) \approx u(0)\left\{1 + \mu\left[\frac{1}{\kappa + u(0)}\frac{\chi^2}{2!} + \frac{\mu\kappa}{(\kappa + u(0))^3}\frac{\chi^4}{4!} + \frac{\mu^2\kappa(\kappa - 6u(0))}{(\kappa + u(0))^5}\frac{\chi^6}{6!}\right]\right\} \tag{13}$$

$$v(\chi) \approx \frac{1}{\gamma}\left[u(0) + \big(1 - u(0)\big)\chi - u(\chi)\right] \tag{14}$$

The dimensionless current is given by

$$\psi \approx \frac{1}{\gamma}[1 - u(0)] \tag{15}$$

The unknown parameter $u(0)$ can be obtained by using the Ying Buzu Shu algorithm, which is given below with a basic idea of these algorithm.

3.1 Basic Idea of Ying Buzu Shu algorithm

Ref. [15] gives a brief overview of the Ying Buzu Shu algorithm, which is currently and frequently used to solve nonlinear oscillators [16,17] and fractal vibration systems [18,19]. Consider the second-order nonlinear differential equation of the form

$$u''(\chi) + f(u(\chi)) = 0 \tag{16}$$

The boundary conditions for the above equation are

$$u'(0) = \alpha = 0 \tag{17}$$

$$u(1) = \beta = 1 \tag{18}$$

From the above result , $u(0)$ can be obtained using Ying algorithm [15] which is given in the next section. Now, consider two initial guesses

$$u_1(0) = a_1 \text{ and } u_2(0) = a_2 \tag{19}$$

where a_1 and a_2 are taken as initial guess values which is less than one. By using the analytical expression of $u(\chi)$ which is obtained from Taylor's series method and the initial guess $u_1(0)$ and $u_2(0)$, we can obtain the terminal values at $\chi = 1$.

$$u_1(1) = \beta_1 \tag{20}$$

$$u_2(1) = \beta_2 \tag{21}$$

According to the Ying Buzu Shu algorithm [15,20-22], the initial estimated value can be expressed as

$$u(0)_{est} = a_3 = \frac{u_1(0)\big(u(1) - u_2(1)\big) - u_2(0)\big(u(1) - u_1(1)\big)}{\big(u(1) - u_2(1)\big) - \big(u(1) - u_1(1)\big)} = \frac{a_1(\beta - \beta_2) - a_2(\beta - \beta_1)}{(\beta - \beta_2) - (\beta - \beta_1)} \tag{22}$$

Using the above result, the terminal value $u_3(1)$ can be obtained and verified, such that $|u(1) - u_3(1))| \leq \varepsilon$, where ε is the smallest number. Suppose $|u(1) - u_3(1))| > \varepsilon$, we can take the next iteration in the algorithm for improving the accuracy of the solution.

3.2. Solution of nonlinear equation using Ying Buzu Shu algorithm

The values of $u(0)$ in the equation (13) can be obtained using Chinese algorithm. By taking one of the experimental value of parameters $\mu = 5$ and $\kappa = 5$ the equation (13) can be written as follows:

$$u(\chi) \approx u(0)\left\{1 + 5\left[\frac{1}{5 + u(0)}\frac{\chi^2}{2!} + \frac{25}{(5 + u(0))^3}\frac{\chi^4}{4!} + \frac{125(5 - 6u(0))}{(5 + u(0))^5}\frac{\chi^6}{6!}\right]\right\} \tag{23}$$

Let us consider the two initial guesses $u(0)$ in the above Eq. (23) are as follows:

$$u_1(0) = 0.6 \text{ and } u_2(0) = 0.7 \tag{24}$$

Using the above initial guesses, the Eq. (24) leads to

$$u_1(1) = 0.8858 \text{ and } u_2(1) = 1.0268 \tag{25}$$

But one of the given boundary condition is $u(1) = 1$. In the Eq. (25), $u_1(1) < 1$ and $u_2(1) > 1$ at $\chi = 1$. Therefore we can apply the following Ying Buzu Shu algorithm [15] from the Eq. (22), to estimate the $u_3(0)$.

$$u_3(0) = \frac{u_1(0)(u(1) - u_2(1)) - u_2(0)(u(1) - u_1(1))}{(u(1) - u_2(1)) - (u(1) - u_1(1))} = 0.68099 \tag{26}$$

This yields $u_3(1) = 1.0001$ from Eq. (23). Therefore, we can consider $u(0) = 0.68099$. Hence Eq. (13) becomes as follows:

$$u(\chi) \approx 0.68099 + 0.29968\chi^2 + 0.01934\chi^4 - 0.9131 \times 10^{-4}\chi^6 \tag{27}$$

Using Eq. (27), the dimensionless concentration of product for the same values of parameters is as follows:

$$v(\chi) \approx \frac{1}{\gamma}(0.319\chi - 0.2997\chi^2 - 0.0193\chi^4 - 0.91315 \times 10^{-4}\chi^6) \tag{28}$$

The dimensionless current for the corresponding values of parameters is as follows:

$$\psi \approx \frac{0.31901}{\gamma} \tag{29}$$

For various values of parameters, μ and κ, the values of $u(0)$ obtained using the Ying Buzu Shu algorithm are given in Table. 1 and Table. 2.

Table 1. Estimation the value of $u(0)$ using Ying Buzu Shu algorithm for different values of μ when $\kappa = 5$.

μ	Initial guesses of $u(0)$		$u(0)_{est}$ Eq. (22)	Taylor's series $u(1)$ Eq. (13)	Boundary condition $u(1)$ (Eq.(11))	Error % of $u(1)$
	$u_1(0) = a_1$	$u_2(0) = a_2$				
0.1	0.96	1.00	0.9918	1.0000	1.0000	0.00
1	0.90	0.95	0.9213	1.0000	1.0000	0.00
5	0.65	0.70	0.6810	1.0001	1.0000	0.01
10	0.45	0.50	0.4904	1.0001	1.0000	0.01

Table 2. Estimation the value of $u(0)$ using Ying Buzu Shu algorithm for different values of κ when $\mu = 10$.

κ	Initial guesses of $u(0)$		$u(0)_{est}$ Eq. (22)	Taylor's series $u(1)$ Eq. (13)	Boundary condition $u(1)$ (Eq.(11))	Error % of $u(1)$
	$u_1(0) = a_1$	$u_2(0) = a_2$				
0.1	5×10^{-4}	6×10^{-4}	5.67×10^{-4}	1.0004	1.0000	0.04
1	0.1	0.13	0.1147	1.0031	1.0000	0.31
5	0.45	0.5	0.4904	1.0001	1.0000	0.01
10	0.6	0.67	0.6650	1.0000	1.0000	0.00

4. DISCUSSIONS

For the given experimental parameter values, equations (13-15) constitute a new and simple analytical formulation of concentration substrate, product, and current by using the new approach to Taylor's series method and Ying Buzu Shu algorithm with a definite number of terms. Thus, for all given values of the ratio of the diffusion coefficients and enzyme reaction rate parameters, the analytical expressions of concentrations and current can be determined using this technique.

4.1 Validation of analytical results with numerical results

Direct comparison with numerical simulations validates the accuracy of the analytical expressions of concentrations. For this purpose, we generated the numerical results using the MATLAB "bvp4c" (refer to Appendix C) function for the same values for the parameters. Table- 3 demonstrates the comparison of concentrations by this method with the simulation for the experimental values of parameters. The relative error between simulation and analytical data for the substrate and product concentration is 1.05 % and 1.19 %, respectively. The approximate results would be highly accurate if more iterations were used.

Table 3. Comparison of analytical concentration of substrate and product with simulations results for some fixed experimental values of parameters $\mu = 10$, $\kappa = 5$ and $\gamma = 1$.

χ	Concentration of substrate $u(\chi)$		Error %	Concentration of product $v(\chi)$		Error %
	Numerical	Eq. (13) This work		Numerical	Eq. (14) This work	
0	0.4996	0.4904	1.84	0.0000	0.0000	0.00
0.25	0.5276	0.5185	1.72	0.1017	0.0992	2.46
0.50	0.6149	0.6059	1.46	0.1416	0.1393	1.62
0.75	0.7630	0.7614	0.21	0.1133	0.1112	1.85
1	1	1.0001	0.01	0.0000	0.0000	0.00
Average Error %			1.05	Average Error %		1.19

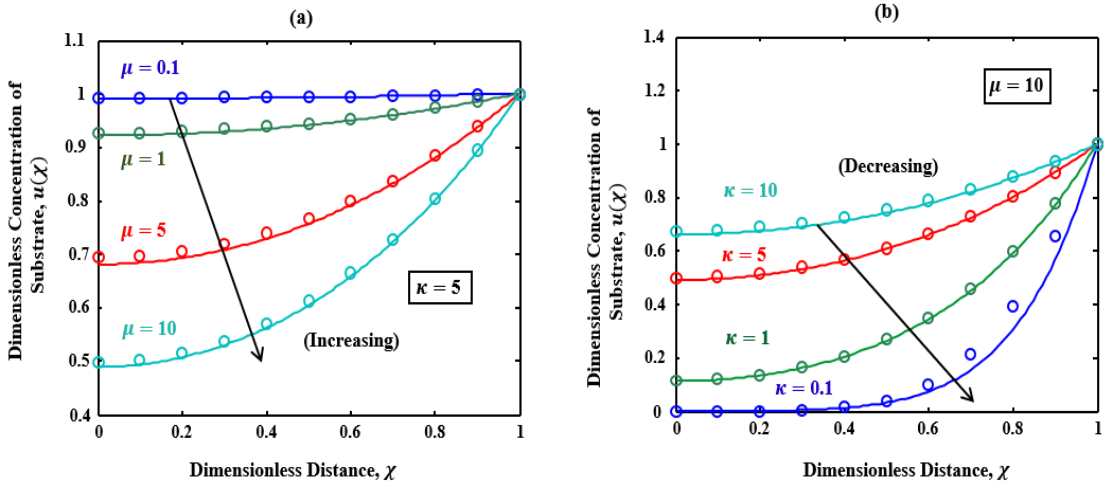

Figure 2. Comparison of analytical expression of substrate $u(\chi)$ (Eq.13) with simulation result. **(a)** For different values of enzyme reaction rate μ, when $\kappa = 5$. **(b)** For different values of saturation parameter κ, when $\mu = 10$.

4.1 Dependence concentration of substrate and product on enzyme reaction rate (μ) *and Michaelis–Menten constant* (κ).

The concentrations of substrate, product, and current density are influenced by a dimensionless parameter called the enzyme reaction rate $\mu(= V_m d^2/D_s S_0)$, as well as the Michaelis–Menten constant $\kappa(= K_m/S_0)$, and the ratio of diffusion coefficients $\gamma(= D_p/D_s)$. The rate of enzyme reaction V_m/S_0 and the diffusion through the enzyme layer (d^2/D_S) determine the dimensionless reaction diffusion parameter μ. If the reaction-diffusion value is $\mu < 1$, the energy devices are dominated by enzyme kinetics. The response is under diffusion control when the reaction-diffusion parameter, μ is greater than unity (μ >1), as shown at high catalytic activity V_m and increased membrane thickness d, or at low initial substrate concentrations S_0 or diffusion coefficient D_s.

The concentration of substrate profiles is shown in Fig.2(a) for different values of enzyme reaction rate, μ. From Fig.2(a) it is noted that the concentration of substrate $u(\chi)$ is uniform when the dimensionless enzyme reaction rate $\mu \leq 0.1$. Also the concentration of substrate $u(\chi)$ at the electrode surface decreases when enzyme reaction rate increases.

The effect of different values of Michaelis–Menten constant for substrate concentration profile is shown in Fig. 2(b). It is observed that decrease in Michaelis–Menten constant, κ leads to decrease in concentration of substrate.

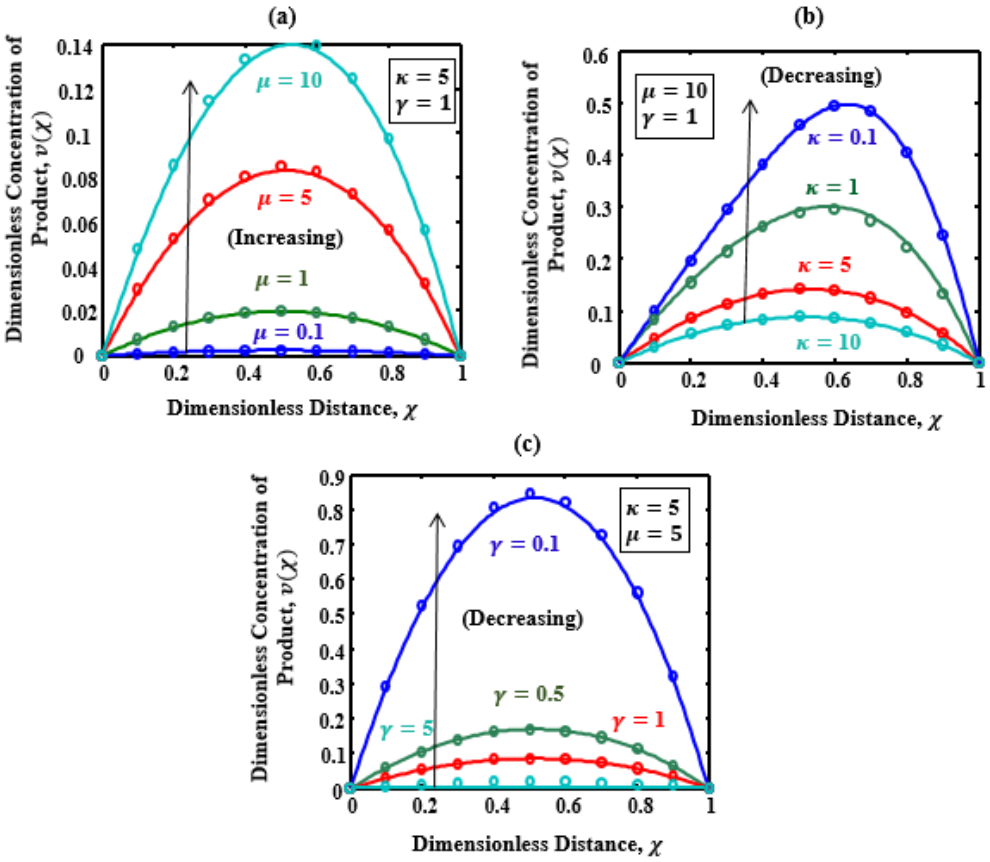

Figure 3. Comparison of analytical expression of $v(\chi)$ (Eq.14) with simulation result **(a).** for different values of μ, when $\kappa = 5$ and $\gamma = 1$. **(b).** for different values of κ, when $\mu = 10$ and $\gamma = 1$ **(c).** for different values of γ, when $\mu = 5$ and $\kappa = 5$.

Figures 3(a-c) illustrate the behavior of the concentration of product for different values of μ, κ and γ. The numerical results show that the effect of increasing values of μ or decreasing the value of κ and γ results in a increasing the product concentration. Also the product concentration increase slowly and reaches the maximum at $\chi =$ 0.5 and then decrease to zero value at $\chi = 1$.

4.2. Impact of the parameters on steady-state current

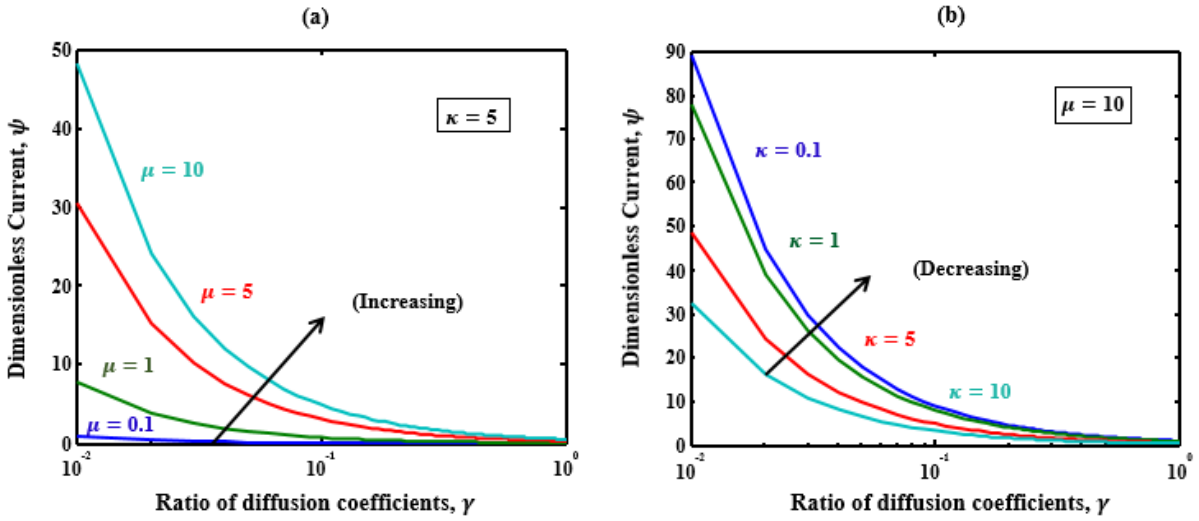

Figure 4. Effect of the dimensionless current, ψ (Eq.15) on the parameters **(a)** γ and μ when $\kappa = 5$, **(b)** γ and κ when $\mu = 10$.

Equation (15) is the new simple, closed- form of current for all values of parameter. But the current is also depend upon the other parameters enzyme reaction rate, μ and Michaelis–Menten constant, κ. At low concentrations of the substrate S_0 the enzyme reaction rate, μ and Michaelis–Menten constant, κ *i*ncreases, which leads to the current fluctuation. That is the steady-state current gains its maximum when there is an increase in the enzyme reaction rate, μ and decrease in the dimensionless Michaelis–Menten constant, κ from the Figs.4(a-b). Also from these figures it is determined that the current flow is decreases gradually when ratio of diffusion coefficient γ increases.

6. CONCLUSIONS

This paper gives a detailed theoretical analysis of amperometric biosensors. The system of non-linear equations in the amperometric biosensor is solved using Taylor's series method with Ying Buzu Shu ancient Chinese algorithm. The solution procedure of this novel method is simple and easy to follow. The substrate, product, and current concentrations were approximated using this method for the first time. The resultant approximation expressions of the concentration were highly accurate compared to reliable numerical results.

ACKNOWLEDGEMENTS
This work was supported by Academy of Maritime Education and Training(AMET), Deemed to be University, Chennai. The authors are thankful to Shri J. Ramachandran, Chancellor, Col. Dr. G. Thiruvasagam, Vice-Chancellor and Dr. M. Jayaprakashvel, Registrar, Academy of Maritime Education and Training (AMET), Deemed to be University, Chennai, Tamil Nadu for their continuous support.

FUNDING
This research received no external funding.

CONFLICT OF INTEREST
The authors declare that they have no conflict of interest

Appendix A: Relationship between $u(\chi)$ and $v(\chi)$

Adding equations (7) and (8) we get,

$$\frac{d^2u(\chi)}{d\chi^2} + \frac{1}{\gamma}\frac{d^2v(\chi)}{d\chi^2} = 0 \quad \text{(A1)}$$

On integrating the above equation, we get the following results:

$$v(\chi) = -\frac{1}{\gamma}u(\chi) + C_1\chi + C_2 \quad \text{(A2)}$$

Using the boundary conditions (9 and 10), the unknown constants $C_1$and C_2can be obtained as follows:

$$C_1 = \frac{1}{\gamma}(1 - u(0)) \quad \text{(A3)}$$

$$C_2 = \frac{1}{\gamma}(u(0)) \quad \text{(A3)}$$

Therefore,

$$v(\chi) = \frac{1}{\gamma}(u(0) + (1 - u(0))\chi - u(\chi)) \quad \text{(A4)}$$

Appendix B: Analytical solution of nonlinear equation Eq. (7) using Taylor's series method.

Consider the Taylor's series solution at $\chi = 0$ for the Eq. (7) as follows:

$$u(\chi) = u(0) + u'(0)\frac{\chi}{1!} + u''(0)\frac{\chi^2}{2!} + u^{(3)}(0)\frac{\chi^3}{3!} + u^{(4)}(0)\frac{\chi^4}{4!} + \ldots\ldots \quad \text{(B1)}$$

And using the boundary condition (Eq. 9), and successive derivative of Eq. (7), we get the following results.

$$u'(0) = 0 \quad \text{(B2)}$$

$$u''(0) = \frac{\mu u(0)}{\kappa + u(0)} \quad \text{(B3)}$$

$$u^{(3)}(0) = 0 \quad \text{(B4)}$$

$$u^{(4)}(0) = \frac{\mu^2\kappa u(0)}{(\kappa + u(0))^3} \quad \text{(B5)}$$

$$u^{(5)}(0) = 0 \quad \text{(B6)}$$

$$u^{(6)}(0) = \frac{\mu^3\kappa u(0)(\kappa - 6u(0))}{(\kappa + u(0))^5} \quad \text{(B7)}$$

Therefore, Eq. (B1) becomes,

$$u(\chi) \approx u(0)\left\{1+\mu\left[\frac{1}{\kappa+u(0)}\frac{\chi^2}{2!}+\frac{\mu\kappa}{(\kappa+u(0))^3}\frac{\chi^4}{4!}+\frac{\mu^2\kappa(\kappa-6u(0))}{(\kappa+u(0))^5}\frac{\chi^6}{6!}\right]\right\} \quad \text{(B8)}$$

From Eq. (A5), $v(\chi)$ can be expressed as follows:

$$v(\chi) \approx \frac{1}{\gamma}[u(0)+(1+u(0))\chi-u(\chi)] \quad \text{(B9)}$$

Appendix C: Matlab program for the nonlinear equations (7) and (8).

```
function chinese_num
m = 0;
x = [0:0.1:1];
t=linspace(0,1);
sol = pdepe(m,@pdex4pde,@pdex4ic,@pdex4bc,x,t);
u1 = sol(:,:,1);
u2 = sol(:,:,2);
figure
plot(x,u1(end,:))
title('u1(x,t)')
xlabel('Distance x')
ylabel('u1(x,2)')
%---------------------------------------------------------------
figure
plot(x,u2(end,:))
title('u2(x,t)')
xlabel('Distance x')
ylabel('u2(x,2)')
% --------------------------------------------------------------
function [c,f,s] = pdex4pde(x,t,u,DuDx)
c = [1;1];
f = [1;1].*DuDx;
mu=5;
k=5;
r=5;
F1 =-mu*(u(1))/((u(1)+k));
F2 =(mu/r)*(u(1))/((u(1)+k));
s=[F1;F2];
% --------------------------------------------------------------
function u0 = pdex4ic(x)
%create  initial conditions
u0 = [1;1];
```

```
% ------------------------------------------------------------
function[pl,ql,pr,qr]=pdex4bc(xl,ul,xr,ur,t)
%create  boundary conditions
pl = [0;ul(2)];
ql = [1;0];
pr = [ur(1)-1;ur(2)];
qr = [0;0];
```

References

1. Y. Ogino, K. Takagi and K. Kano, *J. Electroanal. Chem*., 396 (1995) 517.
2. T. Ikeda and K. Kano, *J. Biosci. Bioeng*., 92 (2001) 9.
3. L. Rajendran and G. Rahamathunissa, *J. Theor. Comput. Chem*., 7 (2008) 113.
4. A. Eswari and L. Rajendran, *J. Electroanal. Chem*., 641 (2010) 35.
5. L. Rajendran and S. Anitha, *Electrochim. Acta* 102 (2013) 474.
6. P.N. Bartlett, C.S. Toh, E.J. Calvo, V. Lexer, Modelling Biosensor Responses, in: P.N. Bartlett (Ed.), Bioelectrochemistry: Fundamentals, Experimental Techniques and Applications, Wiley, (2008) Chichester, England.
7. D. Britz, R. Baronas, E. Gaidamauskait, and F. Ivanauskas, *Nonlinear Anal. Model Control,* 14 (2009) 419.
8. O. Stikoniene, F. Ivanauskas and V. Laurinavicius, *Talanta*., 81 (2010) 1245.
9. A. Meena, and L. Rajendran, *J. Electroanal. Chem.*, 644 (2010) 50.
10. W.E. Morf, P.D. van der waal, E. Pretsch, and N.F. de Rooij, *J. Electroanal. Chem*., 657 (2011) 1.
11. W.E. Morf, P.D. van der waal, E. Pretsch, and N.F. de Rooij, *J. Electroanal. Chem*., 657 (2011) 13.
12. V. Aseris, R. Baronas and J. Kulys, *J. Electroanal. Chem*., 685 (2012) 63.
13. F. Achi, S. Bourouina-Bacha, M. Bourouina and A. Amine, *Sens. Actuators B*, 207 (2015) 413.
14. O.M. Kirthiga and L. Rajendran, *J. Electroanal. Chem*., 751 (2015) 119.
15. J. H. He, *Int. J. Mod. Phys B*, 20 (2006) 1141.
16. C.H. He, C. Liu, J.H. He and A. H. Shirazi, Facta Universitatis: *Mechanical Engineering,* 19 (2021) 229.
17. J.H. He, W.F. Hou, N. Qie, K.A. Gepreel, A.H. Shirazi and H.M. Sedighi, *Facta Universitatis-Series Mechanical Engineering*, 19 (2021) 199.
18. C.H. He, C. Liu and K.A. Gepreel, *Fractals,* 29 (2021) 2150117.
19. J. H. He, *J. Low Freq. Noise Vib. Act. Control*., 38 (2019) 1252.
20. J. H. He, *Results Phys*., 15 (2019) 102546.
21. J. H. He, *Appl. Math. Mech*. (Engl. Ed.,) 23 (2002) 1407.
22. Ji Huan He, Yusry O. and El Dib, *J. Math. Chem.*, 59 (2021) 1139.
23. B Manimegalai, L Rajendran and MEG Lyons, *Int. J. Electrochem. Sci*., 16 (2021).
24. Abdul-Majid Wazwaz, *Optik*, 207 (2020) 164457.
25. K Nirmala, B Manimegalai, and L Rajendran, *Int. J. Electrochem. Sci.*, 15 (2020) 5682.
26. R. Joy Salomi, S. Vinolyn Sylvia, and D. Gowthaman, *Int. J. Adv. Sci. Eng. Inf. Technol*., 29 (2020) 311.
27. M Chitra Devi, L Rajendran, Ammar Bin Yousaf and C Fernandez, *Electrochim. Acta*, 243 (2017) 1.
28. S Vinolyn Sylvia, R Joy Salomi, L Rajendran and Marwan Abukhaled, *J. Math. Chem.*, 59 (2021) 1332.
29. Ramu Usha Rani, Lakshmanan Rajendran and Michael EG Lyons*, J. Electroanal. Chem*., 886

(2021) 115103.
30. L Rajendran R Swaminathan , K Venugopal, M Rasi , M Abukhaled, *Quim. Nova*, 43 (2019) 58. L Rajendran, R Swaminathan, MC Devi , A Closer Look of Nonlinear Reaction-diffusion Equations, *Nova Science Publishers*, (2020), Hauppauge, NY, USA.
31. R Swaminathan, R Saravanakumar, K Venugopal, L Rajendran, *Int. J. Electrochem. Sci*., 16 (2021).
32. R Swaminathan, M Chitra Devi, L Rajendran, K Venugopal, *J. Electroanal. Chem*., 895 (2021) 115527.